This is the accepted manuscript made available via CHORUS. The article has been published as:

The (^{6}Li,^{6}Li^{*}[3.56MeV]) reaction at 100 MeV/u as a probe of Gamow-Teller transition strengths in the inelastic scattering channel

C. Sullivan *et al.*

Phys. Rev. C **98**, 015804 — Published 31 July 2018

DOI: 10.1103/PhysRevC.98.015804

The (^{6}Li, ^{6}Li*[3.56 MeV]) reaction at 100 MeV/u as a probe of Gamow-Teller transition strengths in the inelastic scattering channel

C. Sullivan,[1,2,3] R. G. T. Zegers,[1,2,3,a] S. Noji,[1] Sam M. Austin,[1,3] J. Schmitt,[1,2] N. Aoi,[4] D. Bazin,[1,2] M. Carpenter,[5] J. J. Carroll,[6] H. Fujita,[4] U. Garg,[7] G. Gey,[4] C. J. Guess,[8] T. H. Hoang,[4] M. N. Harakeh,[4,9] E. Hudson,[8] N. Ichige,[10] E. Ideguchi,[4] A. Inoue,[4] J. Isaak,[4] C. Iwamoto,[11] C. Kacir,[8] T. Koike,[10] N. Kobayashi,[4] S. Lipschutz,[1,2] M. Liu,[12] P. von Neumann-Cosel,[13] H. J. Ong,[4] J. Pereira,[1,3] M. Kumar Raju,[4] A. Tamii,[4] R. Titus,[1,2,3] V. Werner,[13] Y. Yamamoto,[4] Y. D. Fang,[4] J. C. Zamora,[1,2,3] S. Zhu,[5] and X. Zhou[12]

[1] *National Superconducting Cyclotron Laboratory, Michigan State University, East Lansing, MI 48824, U.S.A.*
[2] *Department of Physics and Astronomy, Michigan State University, East Lansing, MI 48824, USA*
[3] *Joint Institute for Nuclear Astrophysics: Center for the Evolution of the Elements, Michigan State University, East Lansing, MI 48824, USA*
[4] *Research Center for Nuclear Physics (RCNP), Osaka University, Ibaraki, Osaka 567-0047, Japan*
[5] *Argonne National Laboratory, Argonne, Illinois 60439, USA*
[6] *US Army Research Laboratory, 2800 Powder Mill Road, Adelphi, Maryland 20783, USA*
[7] *Physics Department, University of Notre Dame, Notre Dame, IN 46556, USA*
[8] *Department of Physics and Astronomy, Swarthmore College, Swarthmore, PA 19081, USA*
[9] *KVI-CART, University of Groningen, 9747 AA Groningen, The Netherlands*
[10] *Department of Physics, Tohoku University, Sendai 980-8578, Japan*
[11] *Center for Nuclear Study, University of Tokyo (CNS) RIKEN Campus, 2-1 Hirosawa, Wako, Saitama 351-0198, Japan*
[12] *Institute of Modern Physics, Chinese Academy of Sciences, Lanzhou, China*
[13] *Institut für Kernphysik, Technische Universität Darmstadt, D-64289 Darmstadt, Germany*

(Dated: June 13, 2018)

Background: Inelastic neutrino-nucleus scattering is important for understanding core-collapse supernovae and the detection of emitted neutrinos from such events in earth-based detectors. Direct measurement of the cross sections is difficult and has only been performed on a few nuclei. It is, therefore, important to develop indirect techniques from which the inelastic neutrino-nucleus scattering cross sections can be determined.

Purpose: This paper presents a development of the (^{6}Li, ^{6}Li*[T=1, T_z = 0, 0^+, 3.56 MeV]) reaction at 100 MeV/u as a probe for isolating the isovector spin-transfer response in the inelastic channel(ΔS = 1, ΔT = 1, $\Delta T_z = 0$), from which the Gamow-Teller transition strengths from nuclei of relevance for inelastic neutrino-nucleus scattering cross sections can be extracted.

Method: By measuring the ^{6}Li ejectile in a magnetic spectrometer and selecting events in which the 3.56-MeV γ ray from the decay of the ^{6}Li*[3.56 MeV] state is detected, the isovector spin-transfer selectivity is obtained. High-purity germanium clover detectors served to detect the γ rays. Doppler reconstruction was used to determine the γ energy in the rest frame of ^{6}Li. From the ^{6}Li and 3.56-MeV γ momentum vectors the excitation energy of the residual nucleus was determined.

Results: In the study of the ^{12}C(^{6}Li, ^{6}Li*[3.56 MeV]) reaction, the isovector spin-transfer excitation-energy spectrum in the inelastic channel was successfully measured. The strong Gamow-Teller state in ^{12}C at 15.1 MeV was observed. Comparisons with the analog ^{12}C(^{6}Li,^{6}He) reaction validate the method of extracting the Gamow-Teller strength. In measurements of the ^{24}Mg,^{93}Nb(^{6}Li, ^{6}Li*[3.56 MeV]) reactions, the 3.56-MeV γ peak could not be isolated from the strong background in the γ spectrum from decay of isoscalar excitations. It is argued that by using a γ-ray tracking array instead of a clover array, it is feasible to extend the mass range over which the (^{6}Li, ^{6}Li*) reaction can be used for extracting the isovector spin-transfer response up to mass number $\sim$25 and perhaps higher.

Conclusions: It is demonstrated that the (^{6}Li, ^{6}Li*[3.56 MeV]) reaction probe can be used to isolate the inelastic isovector spin-transfer response in nuclei. Application to nuclei with mass number of about 25 or more, however, will require a more efficient γ-ray array with better tracking capability.

I. INTRODUCTION

Inelastic neutrino-nucleus scattering (INNS) plays an important role during core-collapse supernovae (CCSNe) as it provides a dissipative mechanism by which neutrinos deposit their energy in nuclear matter during the explosion [1–11]. Therefore, to accurately simulate and gain understanding of the details of the late evolution and explosion of massive stars, it is important to have good estimates for the INNS cross section [12–16]. Furthermore, CCSNe produce a strong neutrino signal in the tens-of-MeV range, which can be detected via the products of charged-current (CC) and neutral-current (NC) weak interactions with nuclei in various detector media. However, measurements needed to determine neutrino detector efficiency do not exist for most nuclei, and are

[a] Corresponding author: zegers@nscl.msu.edu

highly uncertain where available due to their small cross sections [17].

One method for studying neutrino-nucleus reactions is direct measurement of neutrino spallation at reactor [18] and synchrotron [19, 20] facilities. Only a few measurements have been performed so far, including the neutrino irradiation of ^{12}C [19, 21]. An alternative approach is via indirect measurements that involve inelastic scattering of other probes, such as (p, p') [22–25] and (e, e') [26, 27]. Such measurements are much easier, and have been used to infer neutral-current neutrino inelastic scattering cross sections in the past [4]. This inference is possible because the cross sections for INNS depend on the same nuclear matrix elements as those that determine the cross sections for the inelastic scattering of hadronic probes. The dominant component of the INNS cross section at astrophysical energies depends on the isovector spin-transfer part of the magnetic dipole transition strength ($M1_{\sigma\tau}$).

The INNS cross section for a transition from an initial (i) to a final (f) state is given by [28] by:

$$\sigma_{i,f}(E_\nu) = \frac{{G_F}^2}{\pi}(E_\nu - \mathit{\Delta} E_{fi})^2 B(M1_{\sigma\tau})_{fi}, \qquad (1)$$

where G_F is the Fermi constant, and E_ν and $\mathit{\Delta} E_{fi}$ are the energy of the incident neutrino and the difference between final and initial nuclear energies, respectively. $B(M1_{\sigma\tau})_{fi}$ is the reduced $M1_{\sigma\tau}$ transition strength in the inelastic channel ($\mathit{\Delta} S = 1$, $\mathit{\Delta} T = 1$, and $\mathit{\Delta} T_z = 0$):

$$B(M1_{\sigma\tau})_{fi} = \frac{1}{2J_i + 1}|\langle f \| \hat{O}(M1_{\sigma\tau}) \| i \rangle|^2, \qquad (2)$$

where J_i the spin of the initial nucleus. $\hat{O}(M1_{\sigma\tau})$ is the corresponding $M1_{\sigma\tau}$ operator,

$$\hat{O}(M1_{\sigma\tau})) = \frac{1}{2}\sum_k \hat{\sigma}(k)\hat{\tau}_0(k), \qquad (3)$$

where $\hat{\sigma} = 2\hat{s}$ and $\hat{\tau} = 2\hat{t}$ are the spin and isospin operators, respectively, and the sum runs over all nucleons in the target. Thus, the allowed component of neutrino-induced nuclear excitations is isovector spin-transfer excitations, with no change in orbital angular momentum.

Reactions mediated by hadronic inelastic scattering induce M1 transitions for which the operator is given by $\hat{O}(M1)$. The electromagnetic magnetic dipole operator is given by

$$\hat{O}(M1) = \sqrt{\frac{3}{4\pi}}\sum_k [g_\ell(k)\hat{\ell}(k) + \frac{1}{2}g_s(k)\hat{\sigma}(k)]\mu_N, \qquad (4)$$

where $\hat{\ell}$ is the orbital angular momentum operator, and g_ℓ (g_s) is the orbital (spin) gyromagnetic factor. Thus, both isovector and isoscalar transitions contribute, as well as non-spin transitions (transitions that involve only change in orbital angular momentum).

The isovector (IV) component of the M1 operator can be rewritten as

$$\hat{O}(M1)_{\mathrm{IV}} = \sum_k \sqrt{\frac{3}{4\pi}}\left(g_\ell^{\mathrm{IV}}\hat{\ell}(k)\hat{\tau}_0(k) + \frac{1}{2}g_s^{\mathrm{IV}}\hat{\sigma}(k)\hat{\tau}_0(k)\right)\mu_N, \qquad (5)$$

with the IV gyromagnetic factors $g_\alpha^{\mathrm{IV}} = (g_\alpha^n - g_\alpha^p)/2$ ($\alpha = \ell$ or s). The isovector spin part of the above IV M1 operator (Eq. (5)) is the same as that of the $M1_{\sigma\tau}$ operator of (Eq. (3)) except for a constant factor. This is furthermore similar to the Gamow-Teller (GT) operators mediating β decay with raising and lowering isospin operators. In the present case, the isospin operator is an isospin projection operator on the third isospin axis. Therefore, in the remainder of this paper we will refer to Gamow-Teller strength, denoted by GT_0, rather than isovector spin M1 dipole strength.

The above discussion indicates that the GT_0 strength, which is needed to infer the INNS cross sections, can be extracted from hadronic probes such as (p, p') only under certain circumstances. Specifically, because the (p, p') reaction is a $J_i^\pi = 1/2^+ \rightarrow J_f^\pi = 1/2^+$ transition and $T_i = T_f = 1/2$, it can induce isovector transitions ($\Delta T = 1$) as well as isoscalar transitions ($\Delta T = 0$) [29]. Therefore, (p, p') can be used to extract GT_0 strength only when the orbital and isoscalar contributions are negligible [4]. This is approximately realized at intermediate incident energies (100-400 MeV), where the central spin-isospin part of the interaction dominates at low momentum transfer [30–32]. In addition, a measurement of the spin-transfer probability (S_{NN}) through polarization-transfer experiments has been used [32] to isolate excitation associated with the transfer of spin. Furthermore, these conditions are reasonably well met for spherically symmetric nuclei with weak or experimentally separable isoscalar responses [33]. However, it would be better to have a probe which is capable of extracting the GT_0 strength from inelastic excitations, without having to be concerned about the orbital and isoscalar contributions. In this work, we investigate $(^6\mathrm{Li}, {}^6\mathrm{Li}^*[T = 1, T_z = 0, J^\pi = 0^+, 3.56\,\mathrm{MeV}])$ reaction as a new reaction probe from which the isovector spin-transfer excitations in the inelastic channel can be directly isolated.

The $(^6\mathrm{Li}, {}^6\mathrm{Li}^*[3.56\,\mathrm{MeV}])$ reaction was first suggested for this purpose in Ref. [34]. It provides access to the GT_0 response of nuclei in an unambiguous manner, as the quantum numbers of the initial and final states guarantee the induced transition of $\mathit{\Delta} S = 1$, $\mathit{\Delta} T = 1$, and $\mathit{\Delta} T_z = 0$. A simplified level diagram of ^{6}Li is shown in Fig. 1 [35]. To identify reactions in which the 0^+ state at an excitation energy of 3.56 MeV is excited, the ^{6}Li particle in the outgoing channel must be tagged with the de-excitation γ ray with $E_\gamma = 3.56\,\mathrm{MeV}$. Although the α threshold is located below the 3.56-MeV state ($Q_\alpha = -1.47\,\mathrm{MeV}$), the α decay from the 3.56-MeV state is blocked, unlike the decay of other states in ^{6}Li, as it is isospin forbidden and violates parity invariance [36, 37]. Instead, this state decays directly to the ground state via γ emission.

Since it has $J^\pi = 0^+$, the branching ratio for decay to the 3^+ state at 2.19 MeV and the feeding from other higher-excited unbound states is negligible [35]. Therefore, the coincidence measurement of a ^{6}Li particle with a 3.56-MeV γ ray provides a clean identification of the desired reaction by isolating the isovector spin-transfer excitations in the inelastic channel. Events in which the ^{6}Li particle is not excited in the reaction are associated with isoscalar excitations. The 3.56-MeV γ ray is not emitted in such events, although γ-rays associated with the isoscalar excitation in the target nucleus create background in the γ spectra.

The extraction of GT transition strengths (B(GT)) from charge-exchange experiments with a variety of hadronic probes at beam energies in excess of about 100 MeV/u has been well established [38–48]. The same method can be used for extracting the GT$_0$ strength in the inelastic channel using the (^{6}Li, ^{6}Li*[3.56 MeV]) reaction. In terms of the reaction mechanism, this reaction, with the exception of minor differences due to the Coulomb forces, is identical to the (^{6}Li,^{6}He) charge-exchange reaction for which the extraction of GT strengths has already been established [49–53].

The extraction of GT transition strength relies on a proportionality between the differential cross section at zero momentum transfer ($\frac{d\sigma}{d\Omega}[q = 0]$) and B(GT) [38]. The proportionality constant is referred to as the unit cross section ($\hat{\sigma}$), which can be calibrated by using GT transitions for which the transition strength is known from β-decay experiments. The calibrated unit cross section can then be applied to all the states excited via GT transitions observed in the spectrum.

In the present work, the ^{12}C(^{6}Li, ^{6}Li*[3.56 MeV]) reaction was used to test the method. Furthermore, measurements on ^{24}Mg and ^{93}Nb were also performed to test the new method for heavier target nuclei. Unfortunately, for the latter two cases, the 3.56-MeV de-excitation γ-ray peak was not resolvable and the isovector spin-transfer excitations could not be separated from other excitations. This was caused by the dominant contributions to the γ spectrum from the γ decay of isoscalar giant resonances excited in the target nucleus. Therefore, the extraction of GT$_0$ matrix elements by using the (^{6}Li, ^{6}Li*[3.56 MeV) reaction presently appears only feasible for relatively light target nuclei, although by using γ-ray tracking techniques the applicability of the probe could possibly be extended to higher masses.

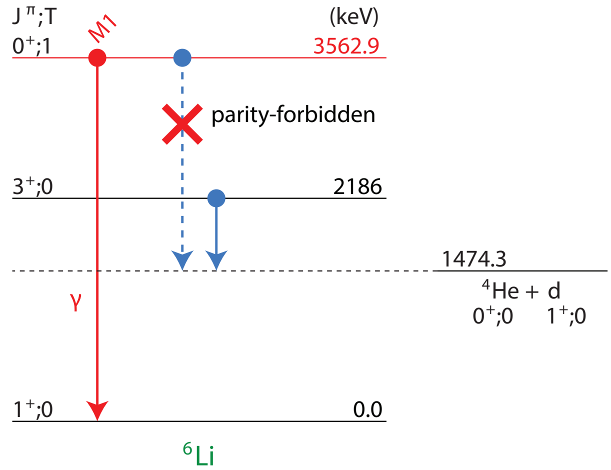

FIG. 1. (color online) A simplified level diagram of ^{6}Li based on Ref. [35]. The α decay of the $J^\pi = 0^+$, $T = 1$ state at $E_x = 3.56$ MeV is isospin and parity forbidden and this state decays to the ground state via γ emission [36, 37].

II. EXPERIMENT

The (^{6}Li, ^{6}Li*[3.56 MeV]) measurements were carried out at the Research Center For Nuclear Physics, Osaka University, Japan. A 100-MeV/u ^{6}Li beam, with a measured energy spread of ~1.5 MeV in full width at half max (FWHM) was accelerated via the coupled operation of the azimuthally varying field (AVF) and ring cyclotrons. The ^{6}Li beam was transported achromatically to the reaction target. A 15.2 mg/cm^2 $^{\text{nat}}$C target was oriented at 22.5° relative to the horizontal plane, yielding an effective thickness of 16.5 mg/cm^2. The rotation of the target was necessary to make sure that the target frames would not block the line of sight between the target and the γ detectors. The energy loss in the target was 0.9 MeV and the energy straggling 0.5 MeV (FWHM). The beam intensity was measured to be ~1 pnA. The target was placed in a scattering chamber, which was surrounded by the Clover Array Gamma-ray spectrometer at RCNP for Advanced research (CAGRA) [54], which consisted of 11 high-purity germanium (HPGe) clover detectors with BGO shields. The ^{6}Li ejectiles were identified and analyzed in the Grand Raiden spectrometer [55], which was placed at 0° relative to the beam axis.

The Grand Raiden focal-plane detectors consisted of two Multi-Wire Drift Chambers (MWDCs), which were used for tracking each particle and determining the positions in the dispersive and non-dispersive directions. The overall detection efficiency for ^{6}Li particles was 74%. By combining the positions in each MWDC, the angles in the dispersive and non-dispersive directions were determined. A calibration measurement by using a sieve-slit was used for the determination of the parameters of a ray-trace matrix for reconstructing scattering angles at the target from position and angle measurements in the focal plane (see, e.g., Ref. [56]). The ion-optics of the spectrometer was tuned to run in under-focus mode [22] to optimize simultaneously the angular resolutions in the dispersive (2.8 mrad (FWHM)) and non-dispersive (10.3 mrad (FWHM)) planes. The momentum reconstruction of the ^{6}Li particles was calibrated by measuring the elastic scattering peak from the ^{93}Nb(^{6}Li,^{6}Li$'$) reaction at several magnetic rigidities.

Three plastic scintillators (thicknesses of 3 mm, 10 mm, and 10 mm) served to extract energy-loss signals and the time of flight (ToF), measured relative to the radio-frequency signal of the cyclotrons. To improve the particle-identification capabilities, a 12-mm aluminum plate was placed in between the second and third scintillators. ^{6}Li particles were stopped in this plate, whereas deuterons and ^{4}He particles from the breakup of ^{6}Li punched through and deposited energy in the third scintillator. Therefore, events in which ^{6}Li breakup occurred could easily be removed in the offline analysis. By combining the energy-loss and ToF signals, ^{6}Li could unambiguously be identified.

The unreacted beam was stopped in a 0° Faraday cup, which was placed ∼12 m downstream of the focal plane. It was shielded to reduce the background for the γ-ray measurement at the target position. The energy of the unreacted beam corresponds to $E_x = 0$ MeV and to prevent the beam from hitting the MWDCs, the detectors were shifted and could cover only $E_x > 10$ MeV. The analysis of the data was carried out up to $E_x = 40$ MeV.

Absolute cross sections were determined on the basis of calibration runs in which the beam intensity was measured with a Faraday cup inserted before the reaction target in between runs. The normalizations from these calibration data were then applied to the other runs. The uncertainty in the absolute cross sections determined with this procedure was estimated at 20%, which was dominated by the read-out accuracy of the Faraday cup in the calibration runs due to a relatively low current.

Eight of the HPGe detectors of the CAGRA array were placed at a laboratory scattering angle of 90° (seven of which were operational) and four were placed at 135°. Each clover detector had four crystals, two at forward scattering angles and two at backward scattering angles. The centroids of the crystals were chosen as the interaction points for the γ rays from which the laboratory angles of the emitted γ rays were determined: 84.3°, 95.8°, 129.0°, and 140.5°. The distance between the target and the centroid of the germanium crystals was 20.8 cm. The angular range covered by a single crystal was 12°.

The Doppler-reconstructed γ-ray energy in the rest frame (c.m.) of the incident particle, $E_\gamma^{\text{c.m.}}$, was obtained from that in the laboratory frame (lab), E_γ^{lab}, by using:

$$E_\gamma^{\text{c.m.}} = \gamma(1 - \beta \cos\theta_\gamma^{\text{lab}})E_\gamma^{\text{lab}}, \qquad (6)$$

where β is the velocity of the excited ^{6}Li particle, and $\theta_\gamma^{\text{lab}}$ is the γ-ray emission angle in the laboratory frame. This reconstructed γ-ray energy peak is broadened ($\varDelta E_\gamma^{\text{c.m.}}$) due to the angular range covered by the finite crystal size, represented by $\varDelta\theta_\gamma^{\text{lab}}$:

$$\left(\frac{\varDelta E_\gamma^{\text{c.m.}}}{E_\gamma^{\text{c.m.}}}\right)_{\theta_\gamma^{\text{lab}}} = \frac{\beta \sin\theta_\gamma^{\text{lab}}}{1 - \beta\cos\theta_\gamma^{\text{lab}}}\varDelta\theta_\gamma^{\text{lab}}. \qquad (7)$$

The contributions to $\varDelta E_\gamma^{\text{c.m.}}$ from the energy resolution of the germanium detectors and the uncertainty in β were negligible. The Doppler-reconstructed γ spectrum was used to identify the photo peak due to the in-flight decay of the 3.56-MeV excited state in ^{6}Li, with a resolution of $\varDelta E_\gamma^{\text{c.m.}} = 250$ keV (FWHM). In combination with the momentum vector of the ^{6}Li particle reconstructed from the spectrometer data, the laboratory momentum vector of the γ rays in the Doppler-reconstructed 3.56-MeV photo peak was used to reconstruct the momentum vector of the ^{6}Li particle prior to the decay by γ emission. The excitation energy of the residual nucleus (e.g. of ^{12}C in the ^{12}C(^{6}Li,^{6}Li*[3.56MeV]) reaction) was then determined in a missing-mass calculation using the momentum vector of the ^{6}Li particle prior to the decay by γ emission. The excitation-energy resolution was almost entirely determined by the uncertainty in the ^{6}Li beam energy (1.5 MeV [FWHM]).

The detection efficiency of CAGRA was determined by using calibrated sources. The energy dependence of the efficiency was simulated in Geant4 [57]. The total efficiency for detecting the photo-peak γ rays associated with the in-flight decay of the 3.56-MeV excited state in ^{6}Li was estimated at (0.44 ± 0.03)%, by taking into account that in the laboratory frame the emission is Lorentz-boosted and the γ-ray energies and yield depend on the emission angle.

The data acquisitions (DAQ) systems for the spectrometer and CAGRA ran independently and events were correlated based on time stamps distributed to each system. The live-time ratios for the DAQ systems were ∼ 0.8 (spectrometer) and ∼ 0.98 (CAGRA). The time difference between correlated events in the spectrometer and CAGRA served to distinguish prompt from random coincidences. By subtracting spectra gated on the random coincidence timings from spectra gated on prompt coincident timing, the true coincidence spectra were created. The prompt-to-random event ratio was 3.3 ± 0.3. The subtraction of random coincidences has been performed for the spectra presented in the following sections.

III. RESULTS AND ANALYSIS

A. The ^{12}C(^{6}Li, ^{6}Li*[3.56MeV]) measurement

The excitation of the strongly excited ^{12}C[15.1 MeV; T=1] state, the analog of the ^{12}B and ^{12}N ground states, was helpful for evaluating the data. The Doppler-reconstructed γ-ray energy spectrum in coincidence with the excitation of this state is shown in Fig. 2. The data between 1500 keV and 5000 keV was fitted with a combination (solid yellow line Fig. 2) of the simulated response from the decay by γ emission of the 3.56-MeV excited state in ^{6}Li and a double-exponential background (dashed blue line). Besides the 3.56-MeV photo peak, the broad bump and tail due to Compton scattering in the germanium detectors are clearly visible around 3 MeV. The four distinct peaks observed in this portion of the spectrum are from the at-rest γ emission from the 2.12-MeV excited state in ^{11}B, populated after the decay by neutron emission from ^{12}C. Because of the four distinct

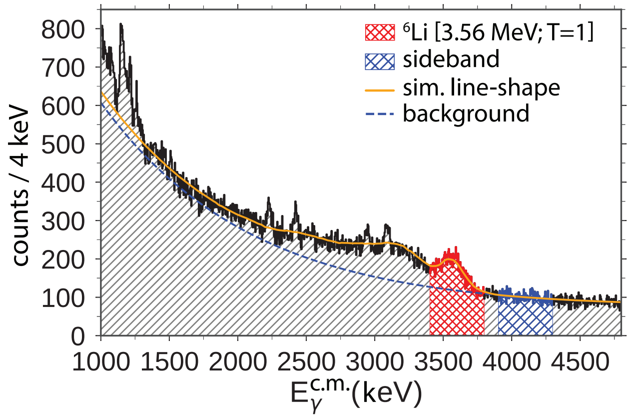

FIG. 2. (color online) The Doppler-reconstructed γ-ray energy spectrum gated on the ^{12}C[15.1 MeV; T=1] excitation. The 3.56-MeV γ line from the decay of the ^{6}Li*[3.56 MeV] excited state is observed and the signal gate (red hatched) and sideband gate for background subtraction (blue hatched) are indicated. The solid yellow line is a fit to the spectrum with a simulated detector response and a double-exponential background (blue dashed line).

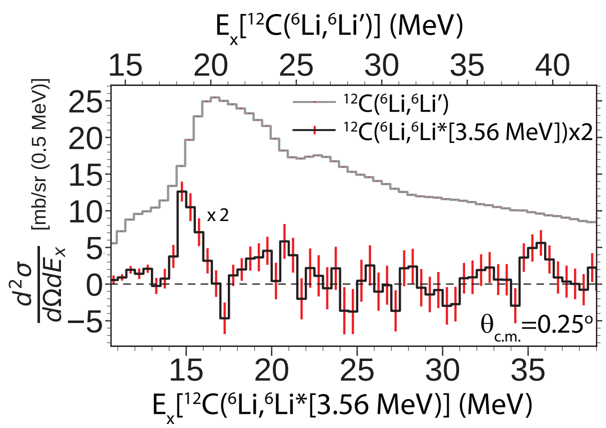

FIG. 3. (color online) Comparison of the ^{12}C inelastic scattering singles and coincidence double differential cross-section spectra at 0.25° for the ^{12}C(^{6}Li, ^{6}Li′) and the ^{12}C(^{6}Li, ^{6}Li*[3.56 MeV]) reactions, respectively. Note that the latter data have been multiplied by a factor of two. See text for details.

scattering angles of the germanium crystals, events associated with this decay appear at four distinct energies in the Doppler-reconstructed spectrum.

By gating on the region $E^{\gamma}_{c.m.}$ = 3.4 MeV - 3.8 MeV in the Doppler-reconstructed γ-energy spectrum (indicated by the red double-hatched region in Fig. 2), events associated with the excitation of the 3.56-MeV excited state in ^{6}Li were selected. Since this region contains background from events not associated with this excitation, data from a side-band between $E^{\gamma}_{c.m.}$ = 3.9 MeV and 4.3 MeV were used to subtract the contribution from the background under the 3.56-MeV peak. This was done

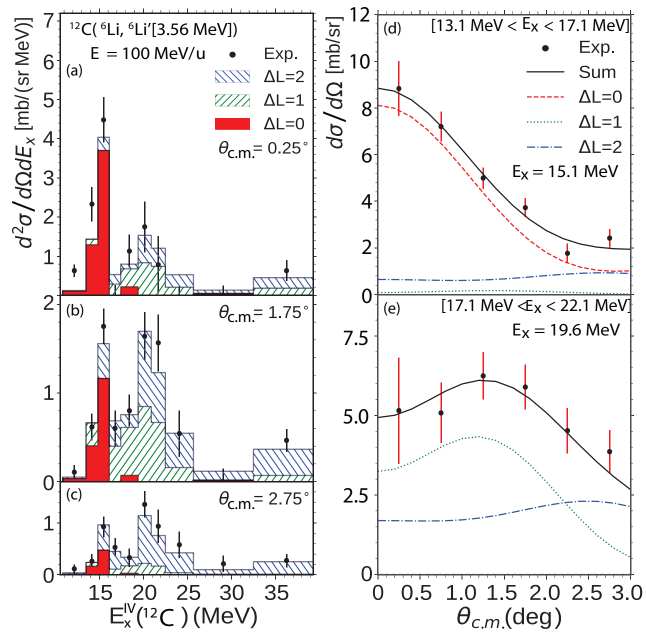

FIG. 4. (color online) Double differential cross sections for the ^{12}C(^{6}Li, ^{6}Li[3.56 MeV]) reaction for 0.5°-wide bins at 0.5° (a), 1.75° (b), and 2.75° (c). Differential cross sections for excitation-energy ranges 13.1-17.1 MeV (d) and 17.1-22.1 MeV (e). The results from the MDA are superimposed (for details see text).

after scaling the number of events in the side band to the estimated number of events under the 3.56-MeV peak as determined by the fit described above.

The procedure as described above for the 15.1-MeV state in ^{12}C was subsequently performed for the ^{12}C excitation-energy spectrum up to 40 MeV. The background-subtracted ^{12}C excitation-energy spectrum gated on the 3.56-MeV excited state in ^{6}Li is shown in Fig. 3 integrated over center-of-mass scattering angles $\theta_{c.m.}$ between 0° and 0.5°. The differential cross sections were corrected for the acceptance of Grand Raiden, the detector live-time ratios, as well as the 3.56-MeV photo-peak efficiency of CAGRA and the ^{6}Li detection efficiency in Grand Raiden. For comparison, the ^{12}C(^{6}Li, ^{6}Li′) singles data are also shown. Note that the excitation energy of the latter spectrum is shifted by 3.56 MeV relative to the former, since it is assumed that the (^{6}Li, ^{6}Li′) singles data are mostly not associated with an excitation of the ^{6}Li particle. The singles data are dominated by isoscalar resonances in ^{12}C and strongly exceeds the cross section for the selective isovector channel.

The double differential cross section for the ^{12}C(^{6}Li, ^{6}Li*[3.56MeV]) reaction as a function of excitation energy in ^{12}C and for three 0.5°-wide center-of-mass scattering-angle bins centered at 0.25°, 1.75°, and 2.75° are shown in Fig. 4(a-c). The spectra have contributions from a variety of excitations associated with different angular-momentum transfer ΔL.

The different multipole contributions to the excitation-energy spectrum were extracted via a multipole-decomposition analysis (MDA) [58]. In the MDA, the differential cross sections in each excitation-energy bin were fitted by a linear combination of theoretical angular distributions associated with different units of orbital angular momentum transfer ($\Delta L = 0, 1$, and 2 were used). The theoretical calculations were performed in Distorted-Wave Born Approximation (DWBA) by using the code FOLD/DWHI [59]. In this code, the Love-Franey effective nucleon-nucleon interaction at 140 MeV [31] was double-folded over the transition densities for the ^{12}C and ^{6}Li inelastic channels. Optical-model potentials for the distorted-wave calculation were obtained by fitting elastic-scattering data for the ^{12}C(^{6}Li,^{6}Li) reaction at 100 MeV/u [60] by using the ECIS [61] code. The best-fit parameters were -60.94 MeV, 1.3725 fm, and 0.9142 fm for the depth (V), radius (r_v), and diffuseness (a_v) of the real Woods-Saxon potential and -22.529 MeV, 1.610 fm, and 0.693 fm for the depth (W), radius (r_w), and diffuseness (a_w) of the imaginary Woods-Saxon potential.

Examples of the MDA for excitation-energy bins from 13.1 MeV to 17.1 MeV and from 17.1 MeV to 22.1 MeV are shown in Figs. 4(d) and (e), respectively. For the former excitation-energy range, the angular distribution is dominated by the $\Delta L = 0$ component associated with the excitation of the 15.1-MeV 1^+ state in ^{12}C. In the latter excitation-energy range, the differential cross section is well described by a combination of comparable $\Delta L = 1$ and $\Delta L = 2$ contributions. The MDA was performed for excitation energies up to 40 MeV and the results are superimposed on the double differential cross sections shown in Figs. 4(a-c). Even though the statistical accuracies of the data are limited, especially at the highest excitation energies, the $T = 1$ 15.1-MeV 1^+ state can clearly be identified, as well as strong dipole and quadrupole contributions at excitation energies up to ~ 25 MeV.

For $N = Z$ ($T = 0$) nuclei such as ^{12}C, it is relatively easy to compare the inelastic ($\Delta T_z = 0$) isovector ($\Delta T = 1$) excitation-energy spectrum with the analog spectrum in the charge-exchange ($\Delta T_z = \pm 1$) channels. The [1^+; $T = 1$; 15.1-MeV] state is the analog of the ground states of ^{12}N and ^{12}B. Indeed, the spectra depicted in Figs. 4(a-c) resemble closely those observed in charge-exchange experiments at similar beam energies on ^{12}C (for example through the (^{6}Li,^{6}He) reaction at 100 AMeV [50] and the (n,p) reaction at 98 MeV [62]) after shifting the excitation energy such that the $T = 1$ 15.1-MeV 1^+ state is at 0 MeV. Note that for $N \neq Z$ ($T \neq 0$) nuclei, such comparisons are in general very difficult, as final states with different isospin in the relevant charge-exchange channel cannot be separated.

From the results for ^{12}C shown in Fig. 4, it is clear that the (^{6}Li,^{6}Li*[3.56MeV]) reaction is suitable for isolating the isovector-spin excitation-energy spectrum in the inelastic channel which establishes this probe as the inelastic analog to spin-transfer charge-exchange reactions. Furthermore, with comparison to the direct ^{12}C(ν,ν') neutrino measurement of Ref. [19], we see that the (^{6}Li,^{6}Li*[3.56MeV]) reaction populates the same states thereby confirming the utility of this probe as an indirect technique for constraining INNS cross sections.

B. Unit cross section

As mentioned in the introduction, the GT transition strengths can be deduced from the measured differential cross sections at zero momentum transfer on the basis of the proportionality between the transition strength and the differential cross section at zero momentum transfer [38, 49]. The proportionality can be expressed as:

$$\frac{d\sigma}{d\Omega}(0^\circ) = \hat{\sigma}_{\rm GT} F(q,\omega) B({\rm GT}), \tag{8}$$

where $\hat{\sigma}_{\rm GT}$ is the unit cross section, $F(q,\omega)$ is a kinematical factor correcting for non-zero momentum and energy transfer, and B(GT) is the GT transition strength. Analogously, the corresponding relation for the present (^{6}Li, ^{6}Li*) reaction is

$$\frac{d\sigma^{(^6{\rm Li},^6{\rm Li}^*)}}{d\Omega}(0^\circ) = \hat{\sigma}_{{\rm GT}_0}^{(^6{\rm Li},^6{\rm Li}^*)} F(q,\omega) B({\rm GT}_0), \tag{9}$$

with $\hat{\sigma}_{{\rm GT}_0}^{(^6{\rm Li},^6{\rm Li}^*)}$ the unit cross section for this reaction and $B({\rm GT}_0)$ the $\Delta T_z = 0$ Gamow-Teller transition strength, i.e. inelastic isovector spin-transfer M1 strength. The factor $F(q,\omega)$ is calculated in the DWBA formalism discussed above by comparing the cross section at finite Q-value and 0° with the cross section at $Q = 0$ and 0° [38].

From the β-decay data of ^{12}B and ^{12}N, the GT transition strengths from the ground states of these nuclei to the ^{12}C ground state are determined to be 0.99 and 0.88, respectively. These transitions are both analogs of the transitions from the ground state to the 15.1 MeV state in ^{12}C. For the determination of the unit cross section $\hat{\sigma}_{{\rm GT}_0}^{(^6{\rm Li},^6{\rm Li}^*)}$, the average of these measurements was adopted. The Gamow-Teller strength for the transition to the 15.1 MeV analog state of the ^{12}B ground state was also calculated via OXBASH [63] using the Cohen-Kurath (8-16)POT interaction in the p-shell-model space [64], and found to be 0.921, which agrees well with the average strength of the β-decay measurements. Utilizing Eq. (9), the ^{12}C(^{6}Li, ^{6}Li*[3.56MeV]) unit cross section was found to be 11.3 ± 2.7 mb/sr (this includes the systematic uncertainty from the measurement as well as the difference in the GT strengths deduced from β decay in each channel). The unit cross section was also determined from the DWBA calculation (11.325 mb/sr) and found to agree with the data. Finally, the unit cross section was also determined from the analog transition in the ^{12}C(^{6}Li,^{6}He) data [50] with a value of ~ 10 mb/sr. Although it was not possible to determine an error from the data presented in Ref. [50], this value is also in good agreement with our present results.

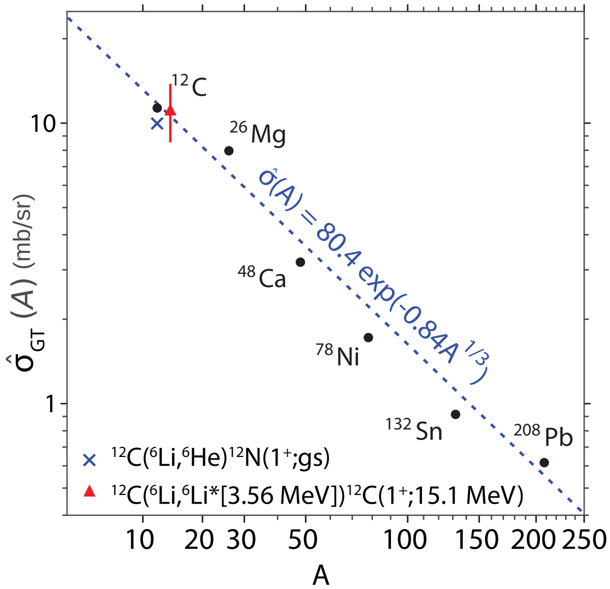

FIG. 5. (color online) GT unit cross section for the (^{6}Li, ^{6}Li*[3.56 MeV]) reaction at 100 MeV/u as a function of target mass number. The red marker is the extracted unit cross section for the ^{12}C(^{6}Li, ^{6}Li*[3.56MeV])^{12}C(15.1 MeV) reaction from the present work. The blue marker refers to the unit cross section from Ref. [50] for the analog transition measured in a ^{12}C(^{6}Li,^{6}He) experiment at 100 MeV/u. The black markers refer to calculated unit cross sections in DWBA and the blue dashed line is a fit to these unit cross sections. For details, see text.

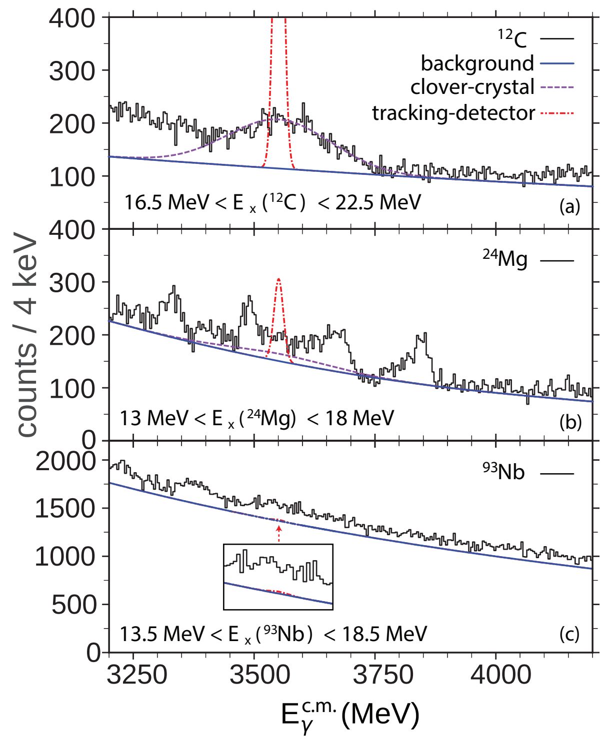

FIG. 6. (color online) Doppler-reconstructed γ-ray spectra for the (^{6}Li, ^{6}Li$'+\gamma$) reaction on ^{12}C (a), ^{24}Mg(b), and ^{93}Nb (c) for the excitation-energy ranges indicated at the bottom of each panel. In (a), the dashed purple line indicates the fitted 3.56-MeV photo-peak and the solid blue line indicates the fitted exponential background. The dot-dashed red line indicates the simulated response if the γ ray position could be measured with a precision of 2 mm. In (b) and (c), the dashed purple line indicates the simulated 3.56-MeV photo-peak assuming one unit of GT strength. The dot-dashed red line indicates the simulated response assuming a position resolution for the γ-ray detection of 2 mm, assuming one unit of GT strength.

The GT unit cross section is expected to decrease as a function of mass number of the target nucleus [38]:

$$\hat{\sigma}_{\mathrm{GT}_0}^{(^6\mathrm{Li},^6\mathrm{Li}')}(A) = N\exp(-xA^{1/3}), \qquad (10)$$

where N and x are parameters that depend on the reaction probe. By using the results for ^{12}C data as described above and additional DWBA calculations for the (^{6}Li, ^{6}Li*[3.56MeV]) reaction on heavier systems, the parameters N and x were determined. The calculations for the heavier target nuclei (^{26}Mg, ^{48}Ca, ^{78}Ni, ^{132}Sn, and ^{208}Pb) were also performed in the same DWBA formalism as described above. The systematic uncertainties are significantly larger as optical-model potentials were not available from elastic scattering data of ^{6}Li at 100 MeV/u for these nuclei and were, therefore, taken from other heavy-ion data [65] or for ^{6}Li at lower beam energy [45]. Nevertheless, a reasonable dependence of the unit cross section for the (^{6}Li, ^{6}Li*[3.56MeV]) reaction at 100 MeV/u as a function of mass number was established, as shown in Fig. 5, with $N = 80$ mb/sr and $x = 0.84$. Clearly, the unit cross section drops rapidly with increasing mass number, which has consequences for the ability to discern the 3.56-MeV peak in the Doppler-reconstructed γ spectrum.

The background under the 3.56-MeV peak in the Doppler-reconstructed γ spectrum is due to γ decay from excited states in the target nucleus as well as γ emission after particle decay of the target. As shown in Fig. 3, isoscalar excitations (predominantly through the (^{6}Li, ^{6}Li[g.s.]) reaction) are much more strongly excited than the isovector excitations. In the excitation-energy region of interest for the isovector excitations, isoscalar giant resonances strongly contribute. The γ decays from these giant resonances are predominantly statistical in nature and have energies ranging up to ~ 8 MeV in the laboratory frame, producing background under the 3.56-MeV peak in the Doppler-reconstructed γ spectrum. The cross section for the excitation of the isoscalar giant resonances is rather independent of mass number [66], which leads to a relative increase in background with increasing mass number due to their decays by γ emission in the Doppler-reconstructed spectrum. This is illustrated in Fig. 6, in which the Doppler-reconstructed spectra for the targets of ^{12}C (see also Fig. 2), ^{24}Mg, and ^{93}Nb targets are shown. For each of the panels, the solid blue line indicates the exponential background and the dashed purple line indicates the photo peak due to the decay from the 3.56-MeV state in ^{6}Li. For the case of ^{12}C, this peak is clearly visible and the purple line is the result of a fit, as discussed above. For the cases of ^{24}Mg and ^{93}Nb no clear peak is observed and the purple line indicates the expected yield for one unit of GT strength from the target nucleus in the excitation-energy windows indicated in each panel. These windows correspond to the region where significant GT$_0$ strength is expected to reside. Clearly, the background is too strong to isolate the 3.56-MeV photo peak. In addition, the background has significant structure due to the fact that the γ detectors were placed at four distinct angles (see above) and γ lines from the decay of the residual in the laboratory frame split up into separate peaks associated with these angles in the Doppler-reconstructed spectrum.

The signal-to-noise (S/N) ratio of the 3.56-MeV peak could be significantly improved by using a γ-ray tracking detector such as GRETINA where the nominal interaction position in the HPGe crystals can be determined to within 2 mm [67–69], which reduces the uncertainty in the Doppler reconstruction. The improvement by being able to better reconstruct the angle of the γ ray was simulated in GEANT4, assuming that the detection efficiencies remained equal. The results are shown by dot-dashed red lines in Fig. 6. Clearly, the use of γ-ray tracking would be very beneficial for improving the S/N ratio of the 3.56-MeV photo peak in the Doppler-reconstructed spectrum. Not only does the tracking detector improve the FWHM of the 3.56 MeV signal, it also smoothes the background as the γ-rays emitted at rest are smeared over a continuous angular distribution. The resulting spectrum would then be similar to the blue background and red simulated line shapes shown in Fig. 6. Thus, with a GRETINA-like tracking detector, experiments on nuclei with mass numbers of around 25 could become feasible. If in addition the photo-peak efficiency is increased (GRETINA achieves an efficiency of $\sim 3\%$ for γ rays around 3.5 MeV, with a geometrical coverage of π sr [69]), additional gains could be achieved. An example of an experiment for which the effectiveness of using a γ-ray tracking array for similar purposes as in the present work can be found in Ref. [70].

IV. CONCLUSIONS

Through an experiment on a ^{12}C target, it has been demonstrated that the (^{6}Li, ^{6}Li*[$T = 1, T_z = 0, J^\pi = 0^+, 3.56\,\text{MeV}$]) reaction at 100 MeV/$u$ can be used to probe the isovector spin-transfer response in the inelastic reaction channel, by tagging the reaction with the 3.56-MeV decay γ ray. This reaction is the neutral-current analog to charge-exchange spin-transfer reactions and can be used to indirectly infer inelastic neutrino-nucleus scattering cross sections. The unit cross section, which defines the proportionality between the Gamow-Teller strength and the differential cross section measured for GT transitions with the (^{6}Li, ^{6}Li*[3.56 MeV]) reaction, was extracted from the measurement of the transition to the 1^+ state at 15.1 MeV in ^{12}C. Its value agreed well with a theoretical estimate in DWBA and with the unit cross section for the analog ^{12}C(^{6}Li,^{6}He)^{12}N(g.s.) reaction.

Since the (^{6}Li, ^{6}Li$'$) reaction strongly excites isoscalar transitions, including the isoscalar giant resonances, the 3.56-MeV γ peak is situated on a strong background from γ-rays from the statistical decay of the isoscalar excitations. Although the isovector spin-transfer cross section drops significantly with increasing mass number, that of the isoscalar resonances remains about equal, which results in a worsening S/N ratio for the 3.56-MeV γ peak with increasing mass number. Consequently, it becomes more difficult to identify and use the 3.56-MeV γ ray for higher-mass nuclei. In the present work, it was not possible to isolate the isovector spin-transfer excitations in the inelastic channel for ^{24}Mg and ^{93}Nb. It was estimated that if an efficient HPGe γ-ray tracking array were to be used, the method for extracting such excitations by using the (^{6}Li, ^{6}Li*[$T = 1, T_z = 0, J^\pi = 0^+, 3.56\,\text{MeV}$]) reaction could extend to nuclei with mass number of about 25 and possibly even higher.

V. ACKNOWLEDGEMENTS

We thank the staff of RCNP for their tireless efforts in preparing the CAGRA array, the Grand Raiden spectrometer and the ^{6}Li beam. CS also thanks Dirk Weisshaar for many helpful discussions in preparing the analysis of the CAGRA data. This material is based on work supported by the National Science Foundation under grant No. PHY-1430152 (JINA Center for the Evolution of the Elements) and No. PHY-1565546, by the US DOE under contract DE-AC02-06CH113567, by the International Joint Research Promotion Program of Osaka University, by DFG under contract SFB 1245, and by Hirose International Scholarship Foundation.

[1] W. C. Haxton, "Neutrino heating in supernovae," Phys. Rev. Lett. **60**, 1999 (1988).

[2] R. Surman and J. Engel, "Neutrino capture by r-process waiting-point nuclei," Phys. Rev. C **58**, 2526 (1998).

[3] G. Martínez-Pinedo, D. J. Dean, K. Langanke, and J. Sampaio, "Neutrino-nucleus interactions in core-collapse supernova," Nucl. Phys. **A718**, 452c (2003).

[4] K. Langanke, G. Martínez-Pinedo, P. von Neumann-Cosel, and A. Richter, "Supernova inelastic neutrino-nucleus cross sections from high-resolution electron scattering experiments and shell-model calculations," Phys. Rev. Lett. **93**, 202501 (2004).

[5] K. Langanke, G. Martínez-Pinedo, B. Müller, H.-T. Janka, A. Marek, W. R. Hix, A. Juodagalvis, and J. M. Sampaio, "Effects of inelastic neutrino-nucleus scattering on supernova dynamics and radiated neutrino spectra," Phys. Rev. Lett. **100**, 011101 (2008).

[6] S. E. Woosley, D. H. Hartmann, R. D. Hoffman, and W. C. Haxton, "The ν-process," Astrophys. J. **356**, 272 (1990).

[7] S. E. Woosley, J. R. Wilson, G. J. Mathews, R. D. Hoffman, and B. S. Meyer, "The r-process and neutrino-heated supernova ejecta," Astrophys. J. **433**, 229 (1994).

[8] S. E. Woosley, A. Heger, and T. A. Weaver, "The evolution and explosion of massive stars," Rev. Mod. Phys. **74**, 1015 (2002).

[9] J. Toivanen, E. Kolbe, K. Langanke, G. Martínez-Pinedo, and P. Vogel, "Supernova neutrino induced reactions on iron isotopes," Nucl. Phys. **A694**, 395 (2001).

[10] A. Hektor, E. Kolbe, K. Langanke, and J. Toivanen, "Neutrino-induced reaction rates for r-process nuclei," Phys. Rev. C **61**, 055803 (2000).

[11] K. Langanke and G. Martínez-Pinedo, "Nuclear weak-interaction processes in stars," Rev. Mod. Phys. **75**, 819 (2003).

[12] K. Langanke and G. Martínez-Pinedo, "The role of electron capture in core-collapse supernovae," Nucl. Phys. **A928**, 305 (2014).

[13] J. Engel, E. Kolbe, K. Langanke, and P. Vogel, "Neutrino induced transitions between the ground states of the $A = 12$ triad," Phys. Rev. C **54**, 2740 (1996).

[14] E. Kolbe, K. Langanke, S. Krewald, and F.-K. Thielemann, "Inelastic neutrino scattering on ^{12}C and ^{16}O above the particle emission threshold," Nucl. Phys. **A540**, 599 (1992).

[15] E. Kolbe, K. Langanke, S. Krewald, and F.-K. Thielemann, "Inelastic neutrino scattering on nuclei and neutrino-nucleosynthesis," Phys. Rep. **227**, 37 (1993).

[16] E. Kolbe, K. Langanke, G. Martínez-Pinedo, and P. Vogel, "Neutrino-nucleus reactions and nuclear structure," J. Phys. G **29**, 2569 (2003).

[17] K. Scholberg, "Supernova neutrino detection," Annu. Rev. Nucl. Part. Sci **62**, 81 (2012).

[18] W. R. Hix, M. Anthony, O. E. B. Messer, and S. W. Bruenn, "Supernova science at spallation neutron sources," J. Phys. G **29**, 2523 (2003).

[19] KARMEN Collaboration, "First observation of the neutral current nuclear excitation $^{12}\mathrm{C}(\nu,\nu')^{12}\mathrm{C}^*(1^+,1)$," Phys. Lett. B **267**, 321 (1991).

[20] KARMEN Collaboration, "Neutrino interactions with carbon: recent measurements and a new test of ν_e, ν_μ universality," Phys. Lett. B **332**, 251 (1994).

[21] R. Imlay, "New results on electron-neutrino carbon scattering and muon-neutrino carbon scattering at LSND," Nucl. Phys. **A629**, 531c (1998).

[22] A. Tamii *et al.*, "Measurement of high energy resolution inelastic proton scattering at and close to zero degrees," Nucl. Instrum. Methods Phys. Res., Sect. A **605**, 326 (2009).

[23] A. Tamii *et al.*, "Complete electric dipole response and the neutron skin in ^{208}Pb," Phys. Rev. Lett. **107**, 062502 (2011).

[24] I. Poltoratska *et al.*, "Pygmy dipole resonance in ^{208}Pb," Phys. Rev. C **85**, 041304(R) (2012).

[25] H. Matsubara *et al.*, "Nonquenched isoscalar spin-$M1$ excitations in sd-shell nuclei," Phys. Rev. Lett. **115**, 102501 (2015).

[26] D. I. Sober, B. C. Metsch, W. Knüpfer, G. Eulenberg, G. Küchler, A. Richter, E. Spamer, and W. Steffen, "Magnetic dipole excitations in the $N = 28$ isotones ^{50}Ti, ^{52}Cr, and ^{54}Fe," Phys. Rev. C **31**, 2054 (1985).

[27] O. Burda *et al.*, "High-energy-resolution inelastic electron and proton scattering and the multiphonon nature of mixed-symmetry 2^+ states in ^{94}Mo," Phys. Rev. Lett. **99**, 092503 (2007).

[28] T. W. Donnelly and R. D. Peccei, "Neutral current effects in nuclei," Phys. Rep. **50**, 1 (1979).

[29] Y. Fujita, B. Rubio, and W. Gelletly, "Spinisospin excitations probed by strong, weak and electro-magnetic interactions," Prog. Part. Nucl. Phys. **66**, 549 (2011).

[30] W. G. Love and M. A. Franey, "Effective nucleon-nucleon interaction for scattering at intermediate energies," Phys. Rev. C **24**, 1073 (1981); "Erratum," Phys. Rev. C **27**, 438 (1983).

[31] M. A. Franey and W. G. Love, "Nucleon-nucleon t-matrix interaction for scattering at intermediate energies," Phys. Rev. C **31**, 488 (1985).

[32] F. T. Baker, L. Bimbot, C. Djalali, C. Glashausser, H. Lenske, W. G. Love, M. Morlet, E. Tomasi-Gustafsson, J. Van de Wiele, J. Wambach, and A. Willis, "The nuclear spin response to intermediate energy protons and deuterons at low momentum transfer," Phys. Rep. **289**, 235 (1997).

[33] A. Richter, "Probing the nuclear magnetic dipole response with electrons, photons and hadrons," Prog. Part. Nucl. Phys. **34**, 261 (1995).

[34] Sam M. Austin, N. Anantaraman, and J. S. Winfield, "Heavy-ion reactions as spin probes," Can. J. Phys. **65**, 609 (1987).

[35] D. R. Tilley, C. M. Cheves, J. L. Godwin, G. M. Hale, H. M. Hofmann, J. H. Kelley, C. G. Sheu, and H. R. Weller, "Energy levels of light nuclei $A = 5, 6, 7$," Nucl. Phys. **A708**, 3 (2002).

[36] A. Csótó and K. Langanke, "Parity-violating α-decay of the 3.56 MeV J^π, $T = 0^+, 1$ state of ^{6}Li," Nucl. Phys. **A601**, 131 (1996).

[37] R. G. H. Robertson, P. Dyer, R. C. Melin, T. J. Bowles, A. B. McDonald, G. C. Ball, W. G. Davies, and E. D. Earle, "Upper limit on the isovector parity-violating decay width of the 0^+ $T = 1$ state of ^{6}Li," Phys. Rev. C **29**, 755 (1984).

[38] T. N. Taddeucci, C. A. Goulding, T. A. Carey, R. C. Byrd, C. D. Goodman, C. Gaarde, J. Larsen, D. Horen, J. Rapaport, and E. Sugarbaker, "The (p, n) reaction as a probe of beta decay strength," Nucl. Phys. **A469**, 125 (1987).

[39] M. Sasano *et al.*, "Gamow-Teller unit cross sections of the (p, n) reaction at 198 and 297 MeV on medium-heavy nuclei," Phys. Rev. C **79**, 024602 (2009).

[40] H. Dohmann *et al.*, "The $(d, {}^2\mathrm{He})$ reaction on ^{96}Mo and the double-β decay matrix elements for ^{96}Zr," Phys. Rev. C **78**, 041602(R) (2008).

[41] R. G. T. Zegers *et al.*, "Extraction of weak transition strengths via the (^{3}He, t) reaction at 420 MeV," Phys. Rev. Lett. **99**, 202501 (2007).

[42] G. Perdikakis *et al.*, "Gamow-Teller unit cross sections for (t, ^{3}He) and (^{3}He, t) reactions," Phys. Rev. C **83**, 054614 (2011).

[43] R. G. T. Zegers *et al.*, "^{34}P(^{7}Li, ^{7}Be + γ) reaction at 100A MeV in inverse kinematics," Phys. Rev. Lett. **104**, 212504 (2010).

[44] R. Meharchand *et al.*, "Probing configuration mixing in ^{12}Be with Gamow-Teller transition strengths," Phys. Rev. Lett. **108**, 122501 (2012).

[45] N. Anantaraman, J. S. Winfield, Sam M. Austin, J. A. Carr, C. Djalali, A. Gillibert, W. Mittig, J. A. Nolen, Jr., and Zhan Wen Long, "(^{12}C, ^{12}B) and (^{12}C, ^{12}N) reactions at $E/A = 70$ MeV as spin probes: Calibration and application to 1^+ states in ^{56}Mn," Phys. Rev. C **44**, 398 (1991).

[46] J. Rapaport and E. Sugarbaker, "Isovector excitations in nuclei," Ann. Rev. Nucl. Part. Sci. **44**, 109 (1994).

[47] W. P. Alford and B. M. Spicer, "Nucleon charge-exchange reactions at intermediate energy," in *Advances in Nuclear Physics*, edited by J. W. Negele and E. Vogt (Springer, Boston, MA, 2002) pp. 1–82.

[48] F. Osterfeld, "Nuclear spin and isospin excitations," Rev. Mod. Phys. **64**, 491 (1992).

[49] H. Ueno *et al.*, "(^{6}Li, ^{6}He) reaction at 100 MeV/nucleon as a probe of spin-excitation strengths," Phys. Lett. B **465**, 67 (1999).

[50] H. Laurent *et al.*, "Spin-isospin multipole excitations by means of the (^{6}Li, ^{6}He) reaction at 100A MeV," Nucl. Phys. **A569**, 297c (1994).

[51] Sam M. Austin, "Spin isospin strength from heavy ions-stable and radioactive beams," Nucl. Phys. **A577**, 51c (1994).

[52] J. S. Winfield, N. Anantaraman, Sam M. Austin, Z. Chen, A. Galonsky, J. van der Plicht, H.-L. Wu, C. C. Chang, and G. Ciangaru, "Mechanism of the (^{6}Li, ^{6}He) reaction at intermediate energies and its suitability as a spin probe," Phys. Rev. C **35**, 1734 (1987).

[53] N. Anantaraman, J. S. Winfield, Sam M. Austin, A. Galonsky, J. van der Plicht, C. C. Chang, G. Ciangaru, and S. Galès, "(^{6}Li, ^{6}He) reaction as a probe of spin-transfer strength," Phys. Rev. Lett. **57**, 2375 (1986).

[54] E. Ideguchi *et al.*, (2018), to be submitted.

[55] M. Fujiwara *et al.*, "Magnetic spectrometer Grand Raiden," Nucl. Instrum. Methods Phys. Res., Sect. A **422**, 484 (1999).

[56] R. G. T. Zegers *et al.*, "Excitation and decay of the isovector spin-flip giant monopole resonance via the ^{208}Pb(^{3}He, tp) reaction at 410 MeV," Nucl. Phys. **A731**, 121 (2004).

[57] J. Allison *et al.*, "Recent developments in GEANT4," Nucl. Instrum. Methods Phys. Res., Sect. A **835**, 186 (2016).

[58] M. A. Moinester, "Multipole decomposition of Gamow-Teller strength," Can. J. Phys. **65**, 660 (1987).

[59] J. Cook and J. Carr, Computer program FOLD/DWHI, Florida State University (unpublished); based on F. Petrovich and D. Stanley, Microscopic interpretation of ^{7}Li + ^{24}Mg inelastic scattering at 34 MeV, Nucl. Phys. **A275**, 487 (1977); modified as described in J. Cook K. W. Kemper, P. V. Drumm, L. K. Fifield, M. A. C. Hotchkis, T. R. Ophel, and C. L. Woods, ^{16}O(^{7}Li, ^{7}Be)^{16}N reaction at 50 MeV, Phys. Rev. C **30**, 1538 (1984); R. G. T. Zegers, S. Fracasso, and G. Colò (unpublished).

[60] K. Schwarz *et al.*, "Reaction mechanism of ^{6}Li scattering at 600 MeV," Eur. Phys. J. A **7**, 367 (2000).

[61] J. Raynal, Computer program ECIS97 (unpublished).

[62] N. Olsson *et al.*, "The ^{12}C(n, p)^{12}B reaction at E_n = 98 MeV," Nucl. Phys. **A559**, 368 (1993).

[63] B. A. Brown, A. Etchegoyen, N. S. Godwin, W. D. M. Rae, W. A. Richter, W. E. Ormand, E. K. Warburton, J. S. Winfield, L. Zhao, and C. H. Zimmerman, Computer program OXBASH, MSU-NSCL report number 1289.

[64] S. Cohen and D. Kurath, "Effective interactions for the 1p shell," Nucl. Phys. **73**, 1 (1965).

[65] A. Nadasen, M. McMaster, M. Fingal, J. Tavormina, P. Schwandt, J. S. Winfield, M. F. Mohar, F. D. Becchetti, J. W. Jänecke, and R. E. Warner, "Unique ^{6}Li-nucleus optical potentials from elastic scattering of 210 MeV ^{6}Li ions by ^{28}Si, ^{40}Ca, ^{90}Zr, and ^{208}Pb," Phys. Rev. C **39**, 536 (1989).

[66] M. N. Harakeh and A. van der Woude, *Giant Resonances: Fundamental High-Frequency Modes of Nuclear Excitation* (Oxford University Press, New York, 2001).

[67] S. Paschalis *et al.*, "The performance of the Gamma-Ray Energy Tracking In-beam Nuclear Array GRETINA," Nucl. Instrum. Methods Phys. Res., Sect. A **709**, 44 (2013).

[68] T. Lauritsen *et al.*, "Characterization of a gamma-ray tracking array: A comparison of GRETINA and Gammasphere using a ^{60}Co source," Nucl. Instrum. Methods Phys. Res., Sect. A **836**, 46 (2016).

[69] D. Weisshaar *et al.*, "The performance of the γ-ray tracking array GRETINA for γ-ray spectroscopy with fast beams of rare isotopes," Nucl. Instrum. Methods Phys. Res., Sect. A **847**, 187 (2017).

[70] M. Scott *et al.*, "Observation of the isovector giant monopole resonance via the ^{28}Si(^{10}Be, ^{10}B*[1.74 MeV]) reaction at 100A MeV," Phys. Rev. Lett. **118**, 172501 (2017).